JOURNAL OF PROPULSION AND POWER
Vol. 12, No. 6, November–December 1996

Arcjet Thruster Development

M. Auweter-Kurtz,* B. Glocker,† T. Gölz,† H. L. Kurtz,‡ E. W. Messerschmid,§ M. Riehle,† and D. M. Zube¶
Universität Stuttgart, Stuttgart D-70550, Germany

For several years an intensive program has been in progress at the University of Stuttgart to investigate and develop thermal arcjets for propellants including ammonia, nitrogen–hydrogen mixtures simulating hydrazine, and hydrogen. Since hydrogen yields the highest specific impulse I_{sp} and best efficiencies η, special emphasis was placed on this propellant. Arcjet power levels between 0.7–150 kW have been studied, including water- and radiation-cooled laboratory models and flight hardware. Results yielded a maximal attainable I_{sp} as a function of the design and power level and showed that increasing power increased I_{sp}. Radiation-cooled arcjets show better η and I_{sp} than water-cooled devices, but raise technical problems because of the high temperatures of the thrusters, which require the use of special refractory materials. Proper arcjet optimization was done with a thorough thermal analysis, including the propellant flow. A further improvement of these thrusters was reached by regenerative cooling and by optimizing the constrictor contour. The constrictor flow is modeled by a three-channel model, the results of which are compared with experimental data. A new two-dimensional computational fluid dynamics (CFD) approach for hydrogen arcjet thrusters is presented. In 1996 a 0.7-kW ammonia arcjet is scheduled for a flight on the P3-D AMSAT satellite.

Introduction

THE potential availability of high electric power supplies in space resulting from large solar arrays or nuclear reactors, resulted in renewed interest in the thermal arcjet thrusters. This is a relatively simple device in which the propellant is heated directly by an electric arc and expanded through a supersonic de Laval nozzle to convert the thermal energy to kinetic energy to create thrust. Most arcjets are of the constrictor type, consisting of a coaxial electrode system, with the nozzle also functioning as the anode. The arc burns through the cylindrical nozzle throat (constrictor). With a given propellant and power level the constrictor determines the behavior and properties of the arcjet.

After an intense development period in the early 1960s in the U.S. and Europe,[1] arcjet thruster development stopped nearly worldwide for almost 20 years. Work on thermal arcjet thrusters resumed about 10 years ago in the U.S., Japan, and Europe. The first space applications of arcjet thrusters, for both secondary and primary propulsion, are forthcoming: American 1–2-kW hydrazine arcjets are in use for north–south station keeping (NSSK) on several spacecraft,[2] and for primary propulsion a small ammonia arcjet (0.7 kW power), ATOS, built by the Institut für Raumfahrtsysteme (IRS), University of Stuttgart, will be installed on the radio amateur satellite AMSAT P3-D,[3] which will be launched in late 1996. In the U.S. an Air Force space demonstration, ESEX, will fly a 26-kW ammonia arcjet thruster.[4] Future applications include orbit raising, repositioning and maneuvering, and drag compensation of large satellites and space stations.

In Germany, in 1986, the IRS of the University of Stuttgart started the development of thermal arcjet thrusters as part of its electric propulsion program. This article describes these efforts and is arranged in two main parts: analysis and experiments, including the status of the hardware. The experimental section again is structured according to the power classes of the investigated arcjet thrusters, ranging from 0.7 kW to more than 100 kW, and involving different propellants.

Analysis

Three-Channel Model

In a properly working arcjet device, the arc extends as a column through the constrictor, surrounded by a cold gas mantle, and attaches at the diverging, supersonic part of the nozzle. The cold gas layer protects the nozzle throat from the heat load of the hot plasma and is heated by conduction, convection, and radiation. The performance of the arcjet is determined mainly by the constrictor flow. Since the arc attaches to the anode on the diverging part, the ohmic heat input within the expanding nozzle is neglected, and here the flow is assumed to be frozen downstream of the constrictor.

According to the three-channel model (TCM),[5] the flow within the constrictor is divided into three zones (Fig. 1), which are separated by constant temperature lines:

1) The hot, current conducting arc column is characterized by ohmic heating, heat conduction, and radiation loss. Since the constrictor pressure is of the order of 1 bar, it is assumed that $T_e = T_i$ and the energy equation reduces to the well-known Heller–Elenbaas equation.[6]

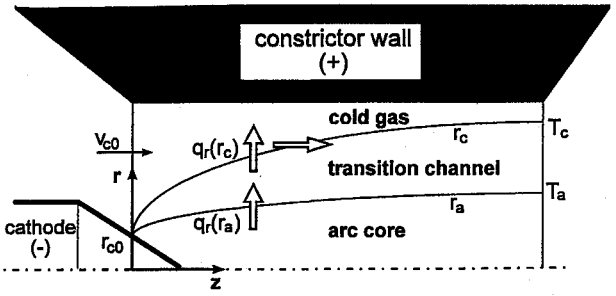

Fig. 1 Schematic of the constrictor region for the TCM.

Received Aug. 31, 1995; revision received Feb. 20, 1996; accepted for publication July 5, 1996.

*Professor, Institut für Raumfahrtsysteme. Member AIAA.
†Research Engineer, Institut für Raumfahrtsysteme. Member AIAA.
‡Research Engineer, Laboratory Supervisor, Institut für Raumfahrtsysteme.
§Professor, Institute Director, Institut für Raumfahrtsysteme. Member AIAA.
¶Research Engineer, Institut für Raumfahrtsysteme; currently at Institut für Thermodynamik und Gebäudeausrüstung, Technische Universität Dresden, Dresden 01062, Germany. Member AIAA.

2) The transition region surrounds the arc channel. It is not current conducting and this region is dominated by dissociation processes. The boundary between these two zones is set to 7000 K. The energy equation for this region is reduced to the heat transport equation under the assumption that radial velocities are small compared to axial ones. The radial heat flux is conducted completely into the cold gas layer.

3) The cold gas zone surrounds the transition zone. The uniform temperature is set to the assumed uniform wall temperature along the constrictor and forms the boundary to the transition zone. It is assumed that most of the cold gas is unaffected by the arc column, the radial heat flux emanating from the transition zone is deposited in the axial flowing cold gas in a small layer around this zone and convected downstream, thus enlarging the transition zone and reducing the cold gas mantle. This model is based on a dual-channel model.[7] The TCM does not need any experimental boundary values except the arc chamber pressure, which has been measured in the water-cooled model described later.

Table 1 shows a comparison of measured and calculated values for a water-cooled thruster. The calculated arc boundaries and mass fractions for a single operating point are presented in Figs. 2 and 3. The calculation shows that the arc core takes only a fraction of the constrictor cross area, which is confirmed by measurements,[8] and at the end of the constrictor about 60% of the propellant is not affected by heating.

Radiation-cooled thrusters require additional assumptions because of the difficulty of accurate arc chamber pressure measurements. Assuming a pressure equal to that in the cold wall thruster and a wall temperature of ~1000 K, the cold gas channel disappears. With this assumption a fairly good correlation with the measured values could still be achieved, the deviations lying in the same range as with cold walls.[8]

Table 1 Comparison of measured and calculated data for the water-cooled arcjet

Mass flow rates ±1%, mg/s	100	100	200	200
Current ±0.5%, A	50.9	151.1	52.5	128.4
Chamber pressure ±1%, mbar	892	1227	1384	1668
Thrust				
Measured ±1%, mN	630	838	882	1165
Calculated, mN	677	897	1079	1260
Discrepancy, mN	47	59	197	95
Voltage				
Measured ±0.5%, V	163.1	142.2	201.4	175.1
Calculated, V	117.0	105.3	155.3	129.3
Discrepancy, V	46.1	36.9	46.1	45.8

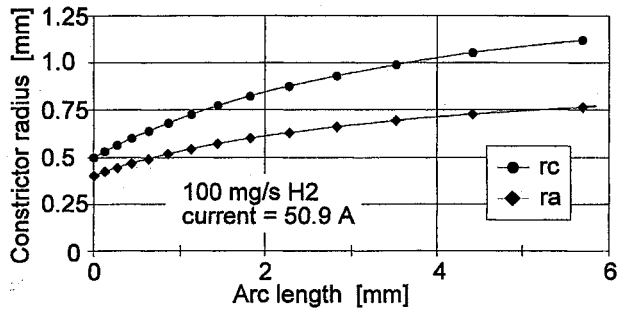

Fig. 2 Boundary of the arc channels.

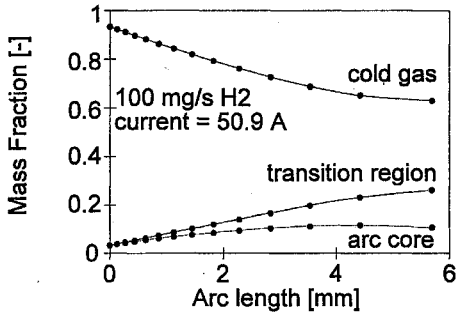

Fig. 3 Mass fraction distribution in the constrictor.

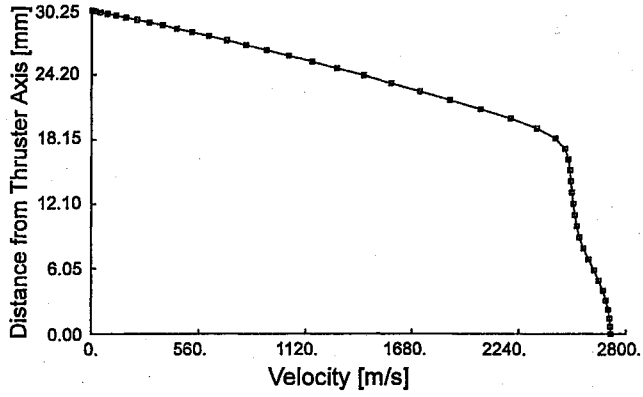

Fig. 4 Velocity profile at the nozzle exit plane with cold hydrogen gas flow.

Detailed Flow Calculations

To overcome the restrictions of the semianalytical TCM, the flowfield of an arcjet is calculated in a detailed CFD code.[9] The actual arcjet flowfield is a three-dimensional viscous reacting turbulent gas flow in a transonic velocity regime with high enthalpy and a current discharge in the gas. For the numerical analysis it is idealized as an axisymmetric laminar viscous reacting gas flow with an electric arc. The effects of current discharge and chemical reactions are taken into account by energy source terms resulting from ohmic heating and heat of reaction. For the calculation, the chemistry module, the current discharge code, and the flow field code were combined to determine the flowfield, the chemical composition, and the current density in the gas. These codes are coupled in the following manner: for a given flowfield the chemical composition is determined. These results are used to calculate the current density. The process is repeated until convergence. The flowfield is discretized with a structured curvilinear mesh with increased line concentration at the boundary walls. Figure 4 shows the axial velocity profile of the cold gas flow with a mass flow rate of 100 mg/s hydrogen at the nozzle exit plane. Peak velocities of almost 2800 m/s were calculated, resulting in an effective exit velocity of 2520 m/s. In contrast to other work performed in the U.S.[10] and Japan,[11] the flowfield was discretized including a region beyond the nozzle exit to compare the numerical results with experimental data taken there.

Experimental Investigations

Arcjets have been tested at power levels from 0.7 to 150 kW. They are tested in different test stands, all equipped with roots pump systems, providing an ambient pressure of ~0.5–10 Pa, depending on the mass flow. All thrusters have a similar starting procedure: A low mass flow rate is set and the current controlled power supply is set to a low current level. Then the discharge is ignited using either the open-circuit voltage of the power supply or by a separate ignition device. The breakdown voltage is typically 1000 V. After ignition the desired operation point is set. Each tank is equipped with a thrust balance of the pendulum type (one arm or parallelogram pendulum), the accuracy of which is better than 1%. If thrust is measured, the thrust balance is calibrated before and after each test. Other measured performance parameters include arc voltage and current (accuracy ±0.5%), mass flow rate, ambient tank pressure, feed line pressure (to monitor changes in thruster behavior), surface temperature distribution, and heat loads to the cooling water, where applicable. The mass flow rates, controlled by

commercial mass flow controllers, are checked during the experiments by high precision weight balances. The accuracy of these measurements is better than 1%. This yields an accuracy of ±1.5% for the I_{sp} and ±2.5% for the efficiency.

The test series showed two trends:

1) Radiation-cooled thrusters generally have a better performance (I_{sp} and η) than water-cooled ones, as a result of energy recovery from the hot thruster housing to the propellant. Further improvements could be obtained with regenerative cooling using hydrogen propellant.

2) Maximal performance data are a function of the geometric size of the devices: The Reynolds numbers affect the viscous and heat transfer losses, and so larger geometries show better performance.

1–2-kW Hydrazine Arcjet Thruster

A collaborative program with industry to develop and build a 1–2-kW arcjet thruster using hydrazine as propellant was started in 1990.[12] Detailed mission analysis revealed good prospects for the application of a 1-kW system for position acquisition of low and medium Earth orbit satellites, and so the project has been focused to this power level.

For the project the IRS is responsible for the arcjet thruster design and development, including arcjet thruster performance and lifetime qualification, and numerical analysis and plasma diagnostics. The industrial partner is providing the design and development of the hydrazine catalyst bed, power supply unit, and tests of the combined system with hydrazine.[12]

The arcjet thruster system requirements are defined as lifetime, >1000 h; operation cycles, >1000; mass flow, 30–15 mg/s (controlled and regulated); mission average I_{sp}, >500 s; input power to PCU, 1.0 kW; and total impulse, >400,000 Ns.

Engineering models of the arcjet thruster components and the catalyst bed have been built and tested. The first hot firing tests with the actual system level unit depicted in Fig. 5 were foreseen for June 1996.

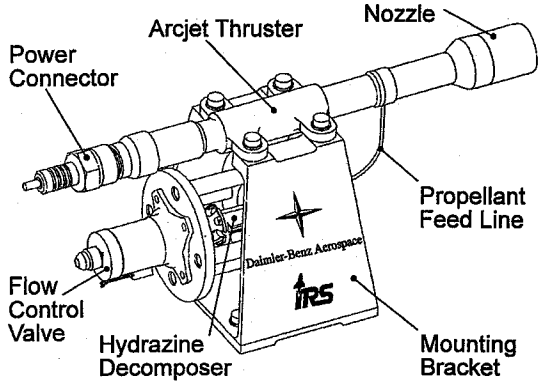

Fig. 5 Hydrazine arcjet thruster with catalyst bed.

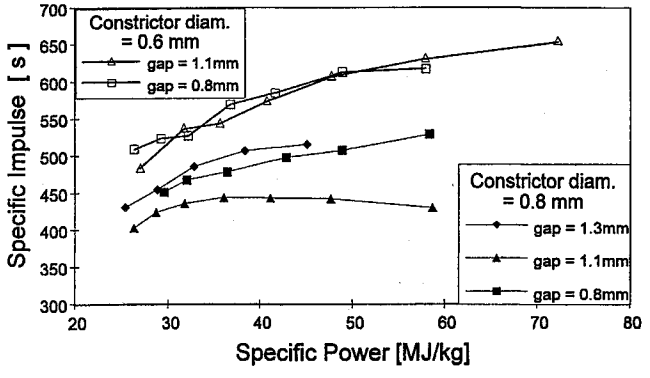

Fig. 6 Specific impulse vs specific power at 1.5 kW for simulated hydrazine. Constrictor diameter for nozzle 1: 0.6 mm and nozzle 2: 0.8 mm.

Tests to evaluate the optimum nozzle configuration were performed with a separate arcjet thruster using 1:2 (mole ratio) nitrogen–hydrogen mixtures. Figure 6 shows (at a constant power level of 1.5 kW) the dominant influence of the constrictor diameter compared to the performance changes coming from the cathode gap variation. The I_{sp} exceeds 600 s at a specific input power of 50 MJ/kg.

Low-Power Hydrogen Arcjets

In 1992 a program was initiated to investigate hydrogen arcjet thruster performance between 1.5–10 kW.[13] For the low-power region, a modified hydrazine laboratory thruster was used with different nozzle geometries and cathode configurations. It is a modular thruster, which is easy to disassemble. The nozzle (anode) and the cathode are made of thoriated tungsten, the housing out of a molybdenum alloy, and the insulator of boron nitride and the seals of graphite foil.

Test runs with this thruster were conducted with mass flow rates between 8–25 mg/s at power levels of 1.0–2.0 kW. With a constrictor diameter of 0.6 mm, the I_{sp} reached 950 s at specific power above 120 MJ/kg for a constant input power of 1.5 kW (Fig. 7a). The thrust efficiency η vs I_{sp} (Fig. 7b) shows relatively high values of more than 45% up to 900 s, but for higher I_{sp}, η drops dramatically and the thruster operation showed incipient instabilities, indicating that the operation limits for this configuration had been reached.

With a larger constrictor diameter of 0.8 mm, the measured I_{sp} was lower and the operational behavior more unstable than with the 0.6-mm constrictor. The variation of the cathode gap within useful limits showed only a minor influence in all cases.

750-W Ammonia Arcjet Thruster

In its series of successful launches and operations of small experimental satellites of the OSCAR series (orbiting satellites carrying amateur radio), the international amateur radio organization AMSAT will launch their P3-D satellite on the second

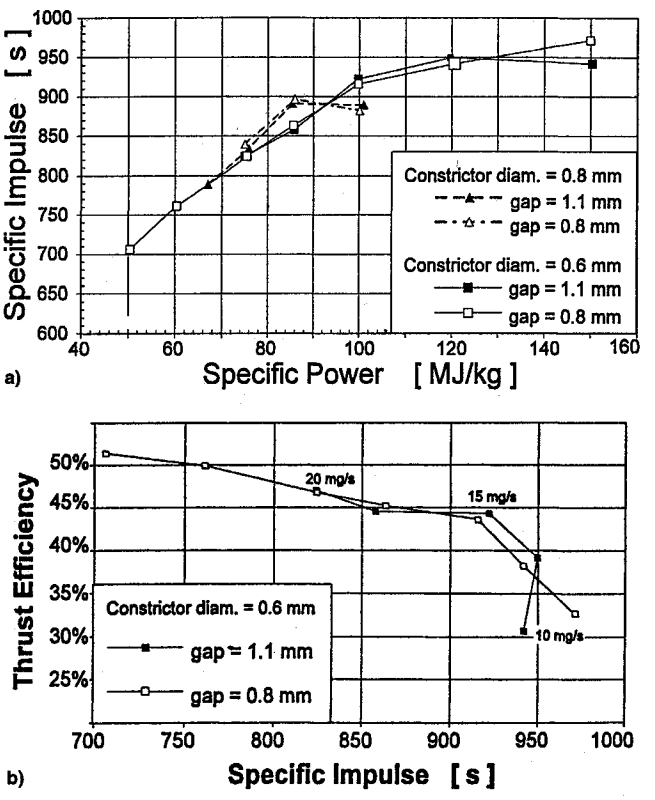

Fig. 7 Low-power hydrogen arcjet thruster at 1.5 kW (constrictor diameter for nozzle 1: 0.6 mm and nozzle 2: 0.8 mm): a) influence of the electrode configuration on the performance and b) thrust efficiency vs specific impulse.

ARIANE 5 launch in late 1996. The satellite will have a mass of about 400 kg and will be launched in a highly elliptical 16-h orbit with a 220-deg argument of the perigee and an inclination of 63.4 deg to eliminate any drift of the argument of the perigee. This orbit will allow the use of the satellite as a transponder for amateur radio satellite broadcasting from regions with high amateur radio density. 650 W of electrical power will be initally available through its solar arrays.

The need to control the orbit inclination and the orbit period within small tolerances for the expected lifetime of the satellite (4–5 years) made the satellite designers consider thermal arcjet thrusters for this purpose.[3] The decision was based on the low thrust levels required and the high fuel efficiency of an arcjet thruster system because of its high I_{sp}. Ammonia was chosen as arcjet propellant to avoid the ground-handling precautions arising from the use of hydrazine. The average electric power available for the arcjet thruster system including all subsystems will be 820 W, the duration for which this power is available depends on the charging status of the spacecraft batteries.[14]

The thruster was dubbed ATOS (arcjet thruster on OSCAR satellite). It is a down-scaled version of the hydrazine arcjet engineering prototype, specially fitted for this purpose. The foreseen lifetime is a total of about 600 h, dictated by the propellant mass flow rate and the propellant mass available on the satellite. Burns lasting 40–60 min are scheduled every third or fourth day. Two lifetime tests have been performed to qualify and evaluate the design. The first one, lasting 670 h, revealed problems with constrictor closure[15] and nozzle throat erosion and necessitated some redesigning of the flight version. The problems were overcome by lowering the anode temperature, as proved by a second, 1010-h lifetest.[14] This leaves the thruster design with a comfortable 167% margin of demonstrated lifetime with regard to the 600-h operation limit on the satellite. The thruster was still operational and in good working condition after this test, which was terminated because additional tests were scheduled with the same thruster. The test results are ATOS flight version data, averaged from 1010 cycle test: arc current, 7.7 A; arc voltage, 97.1 V; electric power input to arcjet, 748 W; power supply efficiency, 93%; mass flow rate, 24 mg/s; thrust, 114 mN; thrust efficiency, 36.2%; specific impulse, 480 s; power supply mass, 2.5 kg; and thruster mass, 480 g. The arcjet input power consumption (the power control unit is current regulated) increased during these 1010 h by about 20% (Fig. 8), indicating that the arcjet system will have to rely on the spacecraft batteries, which essentially limit the length of the arcjet operation.

The lifetime qualification tests of the prototype thruster were also used to qualify most of the other system components. The valves and the ammonia evaporator were purchased already space-qualified through their use in various ammonia resistojet applications on the Meteor spacecraft series.[16] Thermal mass flow controllers (TMFC) are used to guarantee a constant mass flow rate to the arcjet thruster,[3] because the feed line pressure will vary with tank temperature. A contingency feed line with a second, redundant TMFC is used because these devices have not been used in space before, and a malfunction of the TMFC would render the arcjet thruster system useless. The TMFCs work properly only with gaseous ammonia, thus, an electrically heated ammonia vaporizer is included in the system. This vaporizer consumes up to 30 W. The flight thruster was built and delivered, along with the other system hardware, to the AMSAT organization in March 1995, final system integration took place in January 1996.

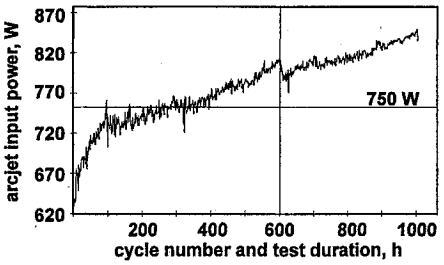

Fig. 8 Power consumption of ATOS during lifetime test.

Medium Power Hydrogen Arcjets

Performance Experiments

Hydrogen arcjets in the power range of 5–25 kW with different cooling systems were evaluated starting with a water-cooled baseline thruster (TT1) with a segmented nozzle.[17] It was compared to the radiation-cooled MARC-1 thruster (medium power arcjet-1). Its design is similar to the low-power hydrazine laboratory model described earlier, but scaled up. The nozzle geometry is the same as that of the water-cooled TT1 to allow a direct comparison. The constrictor diameter is 2.5 mm and the length is 5 mm, the expansion half-angle is 17.5 deg and the area ratio is 1:100.

In Fig. 9 the η and I_{sp} of both thrusters are compared. The performance of the radiation-cooled thruster is better in both parameters: the η is doubled, from ~20 to 40%, and the maximum I_{sp} is raised by ~30%. The gain in performance is a result of the better coupling of the discharge energy to the propellant by its contact with the hot thruster structure. This thermal coupling was proven by a thermal analysis of the radiation-cooled thruster[18] by means of a finite element code,[19] considering unsteady heat conduction, radiation, and convection with nonlinear material properties. For the calculation, the heat load distribution into the anode and cathode was taken from the experimental data, which were determined by thermal measurements of the segmented TT1 thruster.

The thermal modeling of the radiation-cooled thruster was validated by measuring the temperatures of the thruster at three points, one on the anode and two on the housing. As shown in Fig. 10, measured and calculated temperatures agreed well. The temperature on the anode was measured by pyrometer (±0.1%) at given emittance, and the other two points by thermocouple (±3 K). Because the holding bracket, which conducts heat to the thrust balance, was not included in this analysis, the temperatures at measurement points T1 and T2 on the housing deviated slightly with time (Fig. 10). The results showed that for the radiation-cooled thruster an additional ~1.2 kW (12% of the input energy) was transferred to the propellant at a total power input of 10 kW.

The good results with radiation-cooled designs anticipated even better performance with regeneratively cooled nozzles. In a new test series, different nozzles inserts for the medium power arcjet series MARC were compared (Fig. 11).[20] Since the power level was reduced to a maximum of 10 kW, the baseline thruster was revised and the constrictor diameter was reduced to 1.5 mm. MARC-2 represents the purely radiation-

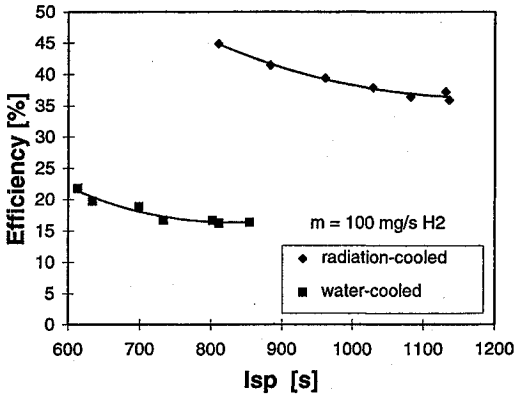

Fig. 9 Performance comparison between water- and radiation-cooled medium-power arcjet thrusters.

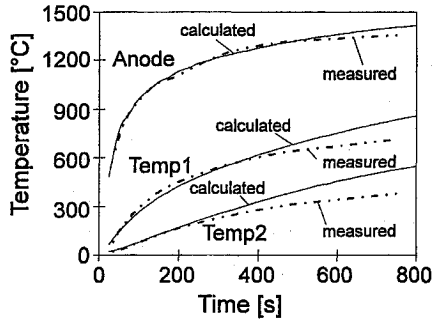

Fig. 10 Measured and calculated temperatures at three surface points.

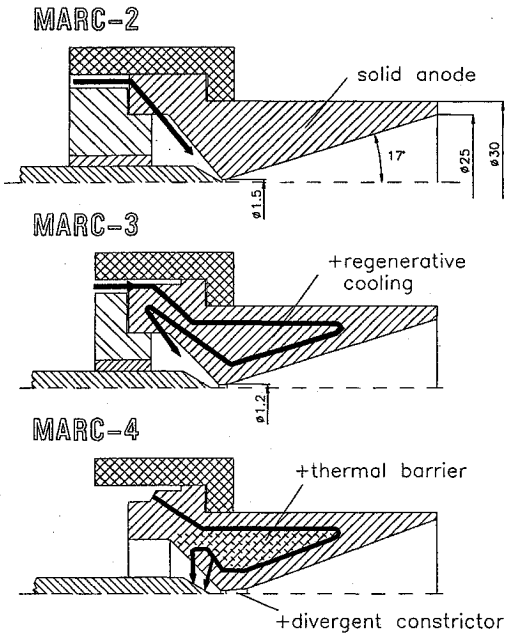

Fig. 11 Propellant flow path for three MARC nozzle inserts.

cooled case. In the MARC-3 thruster the nozzle was regeneratively cooled by directing the propellant flow to the nozzle throat by means of tungsten inserts, also preserving the same propellant injection position and angle. In the MARC-4 version these metal inserts were partly replaced by a ceramic insert to create a thermal barrier and the propellant flow path was modified to minimize the convective heat flux to the rear and outer structure. Additionally, the constrictor shape was altered by introducing a slightly divergent constrictor zone with an initial expansion ratio of 1:3, followed by the divergent nozzle with an overall area ratio of 500. It was expected that the so-called dual-cone constrictor would gain higher efficiencies by recovering part of the frozen flow losses.[21] Figure 12 shows the cooling effect of the regenerative propellant: for the same power and mass flow rate the anode temperature is lowered by more than 250°C and the surface temperature distribution shows significant lower values.

In Fig. 13 the performance data are compared. The regenerative cooling of MARC-3 increased the I_{sp} and η by only ~3%, but with the MARC-4 a further improvement in η of 4–6% could be obtained and 38% at the maximum I_{sp} (1200 s at specific energies of ~180 MJ/kg). The regenerative cooling combined with an optimized constrictor shape offers a great potential to increase hydrogen arcjet performance.

Nozzle Throat Diagnostics

Arcjet optimization benefits from an improved understanding of the constrictor and nozzle flowfields. The water-cooled thruster TT1 was rebuilt to permit optical access into the discharge (Fig. 14). This arcjet consists of stacked water-cooled copper segments, in which the constrictor segment has a hole bored radially through it, giving an optical access to the constrictor as well as enabling pressure measurements in the constrictor. A video camera with microchannel plate intensifier, enabling an exposure time down to 5 ns, was equipped with a magnifying optic and with narrow-band spectral filters.[8]

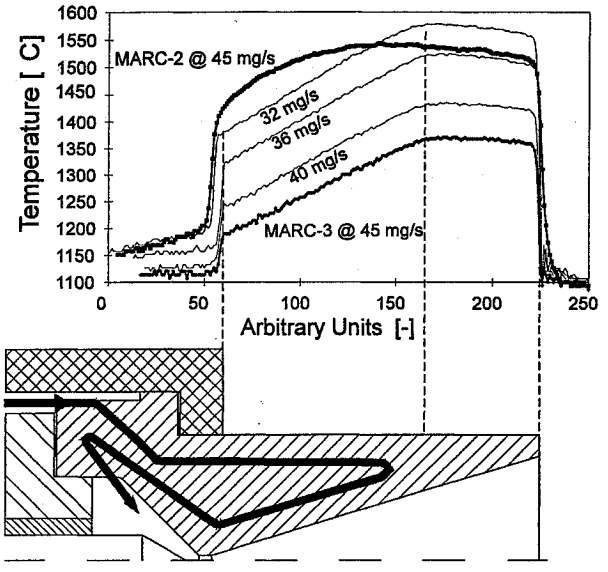

Fig. 12 Comparison of the temperature distribution along the anode axis for MARC-2 and MARC-3 at 5 kW.

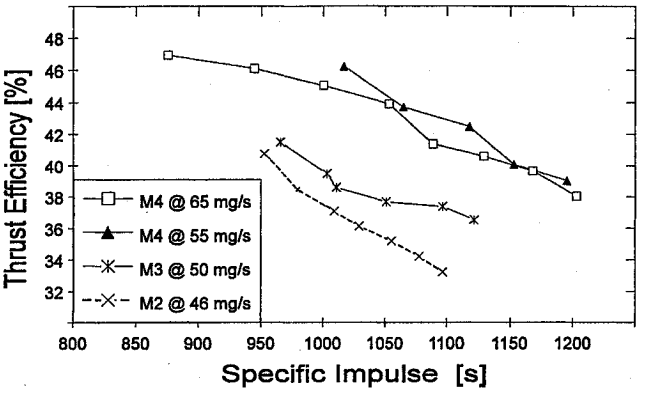

Fig. 13 Thrust efficiency vs specific impulse for the three MARC nozzle inserts.

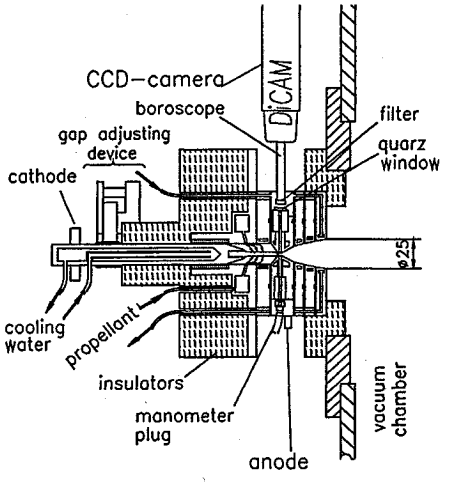

Fig. 14 Experimental setup for the constrictor diagnostic.

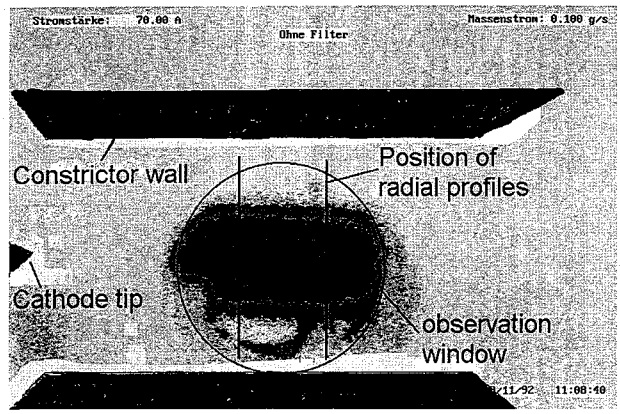

Fig. 15 Arc in the constrictor with the geometric dimensions.

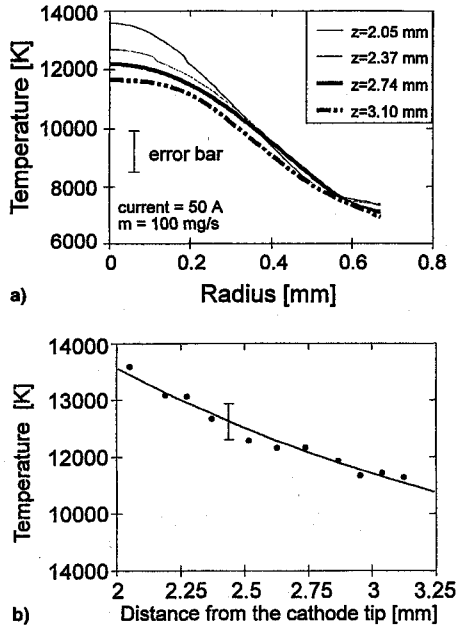

Fig. 16 Temperature distribution in the arc column: a) radial and b) axial distributions of the electron temperature.

Figure 15 shows a typical picture of the arc column. As predicted by the TCM model, the arc does not fill the constrictor. The intensity distribution across the arc was used to calculate the electron temperature distribution, using the continuum emission of the plasma and the Saha equation to calculate the particle densities. Some results are shown for the 50 A and 100 mg/s operation point in Fig. 16a (radial distribution) and Fig. 16b (axial distribution). The electron temperature decreases and the temperature profiles broaden downstream. Under the assumption of local thermal equilibrium the atomic excitation temperature of hydrogen atoms can be derived from the intensity ratio of the H_α and H_β line. The electron and the excitation temperatures coincide well in the arc column center, but deviate at the arc column boundary.[8] This is an indication that the LTE assumption is no longer valid in this region and corona conditions prevail over the Saha conditon.

High-Power Hydrogen Thermal Arcjets

The development of high-power arcjets at the University of Stuttgart began in 1988 with the goal of studying hydrogen arcjets at power levels near 100 kW to serve as electrical loads for 100-kW class space nuclear reactors such as the SP-100.[22] It was also of interest to find out whether such high-power devices would perform better than smaller thrusters. A water-cooled thruster was built and tested first (Fig. 17a), followed by a radiation-cooled device (Fig. 17b).

Water-Cooled Arcjet Thruster

The water-cooled HIPARC (high power arcjet thruster) consisted of a stack of four individually water-cooled anode segments, which together formed a conical nozzle with a half-angle of 20 deg (Fig. 17a). The current input could be measured individually for every anode segment. The nozzle throat diameter could be varied from 2.5 to 6 mm by changing the constrictor segment. The injection angle of the propellant into the arc chamber could be varied through different inserts. This work showed that at this power level tangential injection for a swirl stabilization of the arc has no influence on the thruster performance and behavior. With this thruster and the 6-mm-diam constrictor, a maximum input power of 140 kW could be achieved, and the best performance in operation was observed at a mass flow rate of 200 mg/s and an input power of 100 kW. A thrust value of 3 N led to an I_{sp} of 1500 s at an η of 22%.[23]

Radiation-Cooled Thruster HIPARC-R

Based on the experience gained with the water-cooled thruster, a radiation-cooled 100-kW arcjet device HIPARC-R was designed and built. The design of the cathode/arc chamber/nozzle section was almost identical to the water-cooled thruster with a nozzle throat diameter of 4 mm and a constrictor length-to-diameter ratio of 1. The expansion ratio of the nozzle is 225 compared with 256 with the water-cooled device.

A striking feature of HIPARC-R is the big nozzle body, which is fixed to the thruster housing by six pairs of molybdenum alloy brackets (Fig. 17b). These brackets ensure that the necessary force is exerted on the graphite sealing between nozzle body and thruster housing. This solution was selected for cost- and mass-saving reasons. Cathode and anode are electrically isolated by parts made of boron nitride and a glass ceramic material, respectively.

The thruster was operated with hydrogen mass flow rates ranging from 150 to 300 mg/s. The 100-kW power level could be reached in a steady-state mode with all of these mass flow rates, yielding a specific input power range at 100 kW between 330–670 MJ/kg. As the specific impulse varies almost directly with the specific input power, the best I_{sp} was obtained at the lowest mass flow rate. At 143 mg/s and ~115 kW of input power, a specific impulse of more than 2000 s was measured with a specific power of more than 700 MJ/kg (Fig. 18) and an η of 29%.[24] Temperature data taken using a linear pyrom-

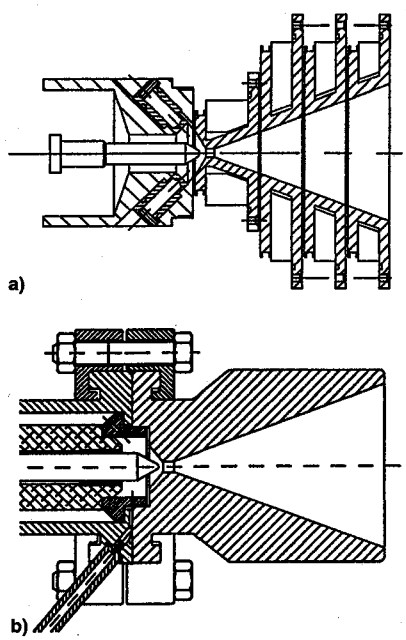

Fig. 17 Cathode/nozzle section: a) water-cooled HIPARC and b) radiation-cooled HIPARC-R.

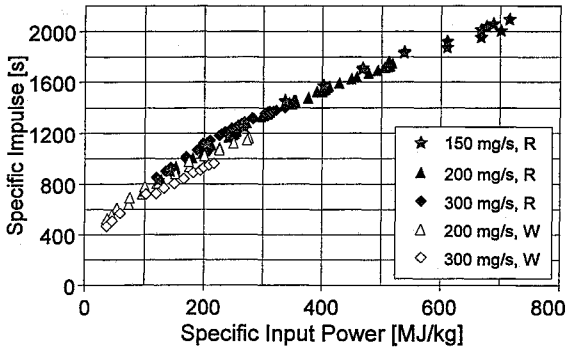

Fig. 18 Specific impulse vs specific input power for the radiation-cooled (R) and the water-cooled (W) thruster, 4-mm constrictor diameter.

eter show maximum temperatures of the uncoated anode of about 2200 K at a steady-state input power of 100 kW.

The improved performance of the radiation-cooled thruster as compared to the water-cooled device resulted from the higher specific input power $P/\dot{m}$ achieved with the radiation-cooled thruster. The specific power of the water-cooled thruster was limited by cooling problems of the constrictor, whereas the radiation-cooled thruster could sustain higher heat loads. This advantage of the radiation-cooled thruster is also shown in Fig. 18, which compares data obtained at mass flow rates of 200 and 300 mg/s with the water-cooled and radiation-cooled thrusters.

Summary

Arcjet thruster studies at the IRS of the University of Stuttgart cover the entire thruster input power range from 700 to over 100 kW with the aim of improving arcjet technology. All hardware work is guided by a combination of thermal and flowfield analyses ranging from the relatively simple TCM to detailed numerical studies. Major achievements to date include the following:

1) Design and flight qualification of a 700-W ammonia thruster to fly on the AMSAT P3-D satellite in late 1996.

2) Evaluation of 1-kW hydrazine thruster systems with an industrial partner. An engineering model is undergoing testing.

3) Demonstration of performance improvements using regenerative cooling on 5- to 10-kW hydrogen arcjets.

4) Successful operation of 100-kW class hydrogen arcjets with both water- and radiation-cooled anodes at specific powers greater than 700 MJ/kg with I_{sp} greater than 2000 s.

The combined theoretical and experimental results have demonstrated the ability to reliably predict the impact of thruster design details (geometry and materials) and operating conditions.

Acknowledgments

The authors are indebted to the following institutions, which sponsored the various thermal arcjet thruster projects during the last years: the European Space Agency ESA/ESTEC, NASA through NASA Lewis Research Center with Grant NAGW-1736, the German Space Agency DARA with Grants 50TA9017, 50TT9404, and 50TT94012, and the German Research Foundation DFG with DFG AU/853-1.

References

[1]Wallner, L. E., and Czika, J., "Arcjet Thrustor for Space Propulsion," NASA TD-2868, June 1965.

[2]Anon., "Electric Propulsion," *Aerospace America*, Vol. 32, No. 12, 1994, p. 58.

[3]Messerschmid, E. W., Zube, D. M., Meinzer, K., and Kurtz, H. L., "Arcjet Development for Amateur Radio Satellite," *Journal of Spacecraft and Rockets*, Vol. 33, No. 1, 1996, pp. 86–91.

[4]Sutton, A. M., Bromaghim, D. R., and Johnson, L. K., "Electric Propulsion Space Experiment (ESEX) Flight Qualification & Operations," AIAA Paper 95-2503, July 1995.

[5]Glocker, B., Schrade, H., and Auweter-Kurtz, M., "Performance Calculation of Arcjet Thrusters—the Three Channel Model," *Proceedings of the 23rd International Electric Propulsion Conference* (Seattle, WA), Vol. 3, Electric Rocket Propulsion Society, Columbus, OH, 1993, p. 1720–1732.

[6]Elenbaas, W., *Physica*, Vol. 1, 1934, pp. 673–688; also Heller, G., *Physica*, Vol. 6, 1935, p. 389–394.

[7]Schrade, H. O., and Sleziona, P. C., "Performance Calculation of an H_2 Arcjet by Means of a Dual Channel Model," *Proceedings of the 20th International Electric Propulsion Conference* (Garmisch, Germany), Deutsche Gesellschaft für Luft- und Raumfahrt, Bonn, Germany, 1988, p. 583.

[8]Glocker, B., "Experimentelle und Theoretische Untersuchungen zur Entwicklung Eines Thermischen Lichtbogentriebwerks der Mittleren Leistungsklasse," Ph.D. Dissertation, Univ. Stuttgart, Germany, 1993.

[9]Gölz, T. M., Auweter-Kurtz, M., and Kurtz, H. L., "High Power Arcjet Experiments and Analysis," 24th International Electric Propulsion Conf., Paper 95-14, Moscow, Russia, 1995.

[10]Miller, S. A., "Multifluid Nonequilibrium Simulation of Arcjet Thrusters," Ph.D Dissertation, Massachussetts Inst. of Technology, Cambridge, MA, 1993.

[11]Fujita, K., and Arakawa, Y., "Anode Heat Loss and Current Distributions in DC Arcjets," *Proceedings of the 23rd International Electric Propulsion Conference* (Seattle, WA), Vol. 3, Electric Rocket Propulsion Society, Columbus, OH, 1993, pp. 1703–1713.

[12]Zube, D. M., Glocker, B., Kurtz, H. L., Kinnersley, M., and Matthäus, G., "Development of a Low Power Radiatively Cooled Thermal Arcjet Thruster," 22nd International Electric Propulsion Conf., Paper 91-042, Viareggio, Italy, 1991.

[13]Riehle, M., Auweter-Kurtz, M., and Kurtz, H. L., "High Specific Impulse Experiments with 1.5 and 5 kW Thermal Arcjets," *Proceedings of the 23rd International Electric Propulsion Conference* (Seattle, WA), Vol. 3, Electric Rocket Propulsion Society, Columbus, OH, 1993, pp. 1934–1948.

[14]Zube, D. M., Messerschmid, E. W., and Dittmann, A., "Project ATOS—Ammonia Arcjet Lifetime Qualification and System Components Test," AIAA Paper 95-2508, July 1995.

[15]Lichon, P. G., and Sankovic, J. M., "Development and Demonstration of a 600 s Mission Average Arcjet," *Proceedings of the 23rd International Electric Propulsion Conference* (Seattle, WA), Vol. 1, Electric Rocket Propulsion Society, Columbus, OH, 1993, pp. 789–803.

[16]Koroteev, A. S., and Rylov, Y. P., "Development and Application of Electrothermal Thrusters on Russian Spacecraft," International Astronautical Federation, Paper 94-S.3.424, Oct. 1994.

[17]Glocker, B., Auweter-Kurtz, M., Gölz, T. M., Kurtz, H. L., and Schrade, H., "Medium Power Arcjet Development," AIAA Paper 90-2531, July 1990.

[18]Glocker, B., and Auweter-Kurtz, M., "Radiation Cooled Medium Power Arcjet Experiments and Thermal Analysis," AIAA Paper 92-3834, July 1992.

[19]Argyris, J., Laxander, A., and Szimmat, J., "Petrov-Galerkin Finite Element Approach to Coupled Heat and Fluid Flow," *Computer Methods in Applied Mechanics*, Vol. 94, No. 2, 1992, pp. 181–193.

[20]Riehle, M., Kurtz, H. L., and Auweter-Kurtz, M., "Investigations of Advanced Medium Power Hydrogen Arcjets," AIAA Paper 95-2507, July 1995.

[21]Butler, G. W., Cassady, R. J., Hoskins, W. A., King, D. Q., and Kull, A. E., "Performance of Advanced Concept Hydrogen Arcjet Anodes," *Proceedings of the 23rd International Electric Propulsion Conference* (Seattle, WA), Vol. 3, Electric Rocket Propulsion Society, Columbus, OH, 1993, pp. 1949–1962.

[22]Mondt, J. F., "SP-100 Space Reactor Power System for Lunar, Mars and Robotic Exploration," International Astronautical Federation, Paper 92-0563, Aug. 1992.

[23]Gölz, T., Auweter-Kurtz, M., and Kurtz, H. L., "100 kW Hydrogen Arcjet Thruster Experiments," AIAA Paper 92-3836, July 1992.

[24]Gölz, T. M., Auweter-Kurtz, M., and Kurtz, H. L., "Development and Testing of a 100 kW Radiation-Cooled Thermal Hydrogen Arcjet Thruster," *Proceedings of the 23rd International Electric Propulsion Conference* (Seattle, WA), Vol. 3, Electric Rocket Propulsion Society, Columbus, OH, 1993, pp. 2079–2088.